Journal of Molecular Structure: THEOCHEM 916 (2009) 159–167

Contents lists available at ScienceDirect

Journal of Molecular Structure: THEOCHEM

journal homepage: www.elsevier.com/locate/theochem

Theoretical study on the detailed reaction mechanisms of carbonyl oxide with formic acid

Bo Long [a,*], Jia-Rong Cheng [a], Xin-feng Tan [b], Wei-jun Zhang [c]

[a] School of Physics and Information Science, Guizhou University for Nationalities, Guiyang 550025, China
[b] College of Photo-Electronics, Chongqing University of Posts and Telecommunications, Chongqing 400065, China
[c] Laboratory of Environment Spectroscopy, Anhui Institute of Optics and Fine Mechanics, Chinese Academy of Sciences, Hefei 230031, China

ARTICLE INFO

Article history:
Received 7 May 2009
Received in revised form 13 August 2009
Accepted 14 September 2009
Available online 17 September 2009

Keywords:
Carbonyl oxide
Formic acid
Reaction mechanisms
B3LYP
CBS-QB3

ABSTRACT

The reaction mechanisms of carbonyl oxide with formic acid are investigated using the B3LYP/6-311G(d,p) and CBS-QB3 theoretical methods. The investigation encompasses the eight complexes formed between carbonyl oxide and formic acid, the initial transition states responsible for the formation of these transitory products including hydroxylated ozonide and hydroperoxymethyl formate, the cleavages of the transitory intermediates and the interconversion between the transitory products and between syn-formic acid anhydride and anti-formic acid anhydride. The calculated results predict that the binding energy of the most stable complex in the eight complexes is −11.0 kcal/mol, which indicates that the formed pre-complexes are of special important for the reaction carbonyl oxide with formic acid. In addition, the barrier heights of the transition states that lead to the hydroxylated ozonide and hydroperoxymethyl formate are −0.5 kcal/mol, −1.3 kcal/mol, respectively, at the CBS-QB3 level of theory, which shows that the two reaction channels contribute to the transitory product formation. In addition, under some circumstances, the cleavages of transitory products result in the formation of the anti-formic acid anhydride, which is in well agreement with experimental predictions. It is noted that splits of hydroxylated ozonide are responsible for the formation of formic acid.

1. Introduction

Carbonyl oxide (H_2COO) is of great importance species in the atmosphere [1]. The unimolecular decompositions and isomerization reactions of the excited carbonyl oxide yield carbonic oxide, carbon dioxide, water, OH, H_2, HCOOH, HCO and oxygen atom [2–5] and thus are the source of the OH radical; On the other hand, the collisionally stabilized Criegee radicals can react with other compounds such as carbonyl compounds, CO, SO_2, O_3, NO_2, NO, HCHO, CH_3 OH, H_2O or HCOOH [6–13], which contributes to the formation of aerosols [14–21].

Carbonyl oxide is produced in the reaction ozone with unsaturated hydrocarbons. The alkene ozonolysis reaction occurs through the so-called Criegee mechanism [22] that the terminal two oxygen atoms in ozone simultaneously add to the C=C bond in the alkene to form the primary ozonide that subsequently undergoes the unimolecular decomposition, yielding a carbonyl oxide and a carbonyl compound. The importance of the carbonyl oxide in atmosphere chemistry is obvious because the amount of the unsaturated hydrocarbons released into atmosphere is larger than 500×10^9 kg C/yr. However, the reaction ozone with unsaturated hydrocarbons is also one of the main sink paths.

Studies reported in the literature [23] have shown that the HC(O)OC(O)H is the main product in the reaction of carbonyl oxide with formic acid. Form the theoretical point of view, the calculated results [24] demonstrated that there were no existed transition states for the reaction carbonyl oxide with formic acid. In this study, we apply to high level ab initio methods to study the reaction mechanisms of carbonyl oxide with formic acid. The work investigates the pre-complexes formed between carbonyl oxide and formic acid to clarify the reaction mechanisms, the concerted reactions carbonyl oxide with formic to lead to the formation of the transitory products and the cleavage of primary transitory products as schematized 1–5 below. Although the importance in atmospheric chemistry may be limited because of the competition of the reaction carbonyl oxide with water vapor, which is in higher concentration in the troposphere, the reaction mechanisms are high interest and valuable, for it is of great help for us to understand the bimolecular reactions of the carbonyl oxide with other compounds, leading to the formation of secondary organic aerosols.

* Corresponding author.
E-mail address: wwwltcommon@sina.com (B. Long).

0166-1280/$ - see front matter Crown Copyright © 2009 Published by Elsevier B.V. All rights reserved.
doi:10.1016/j.theochem.2009.09.028

$$H_2COO + HCOOH \rightarrow H_2COOC(H)(O)OH \quad (1)$$

$$H_2\overline{COOC(H)(O)}OH \rightarrow 2HCOOH \quad (2)$$

$$H_2\overline{COOC(H)(O)}OH \rightarrow HCHO + CO_2 + H_2O \quad (3)$$

$$H_2COO + HCOOH \rightarrow H_2C(OOH)OC(H)O \quad (4)$$

$$H_2C(OOH)OC(H)O \rightarrow H_2O + HC(O)OC(O)H \quad (5)$$

2. Theoretical methods

The electronic structure calculations were accomplished using the Gaussian 03 [25] software. The spin-unrestricted form of the B3LYP functional was carried out to judge whether it would describe the electronic structure of the transition states founded in this study than the spin-restricted functional. The test results show that the UB3LYP and B3LYP energies, frequencies and geometrical parameters are identical. Therefore, All geometries were optimized at the B3LYP/6-311G(d,p) level of theory and then the frequencies

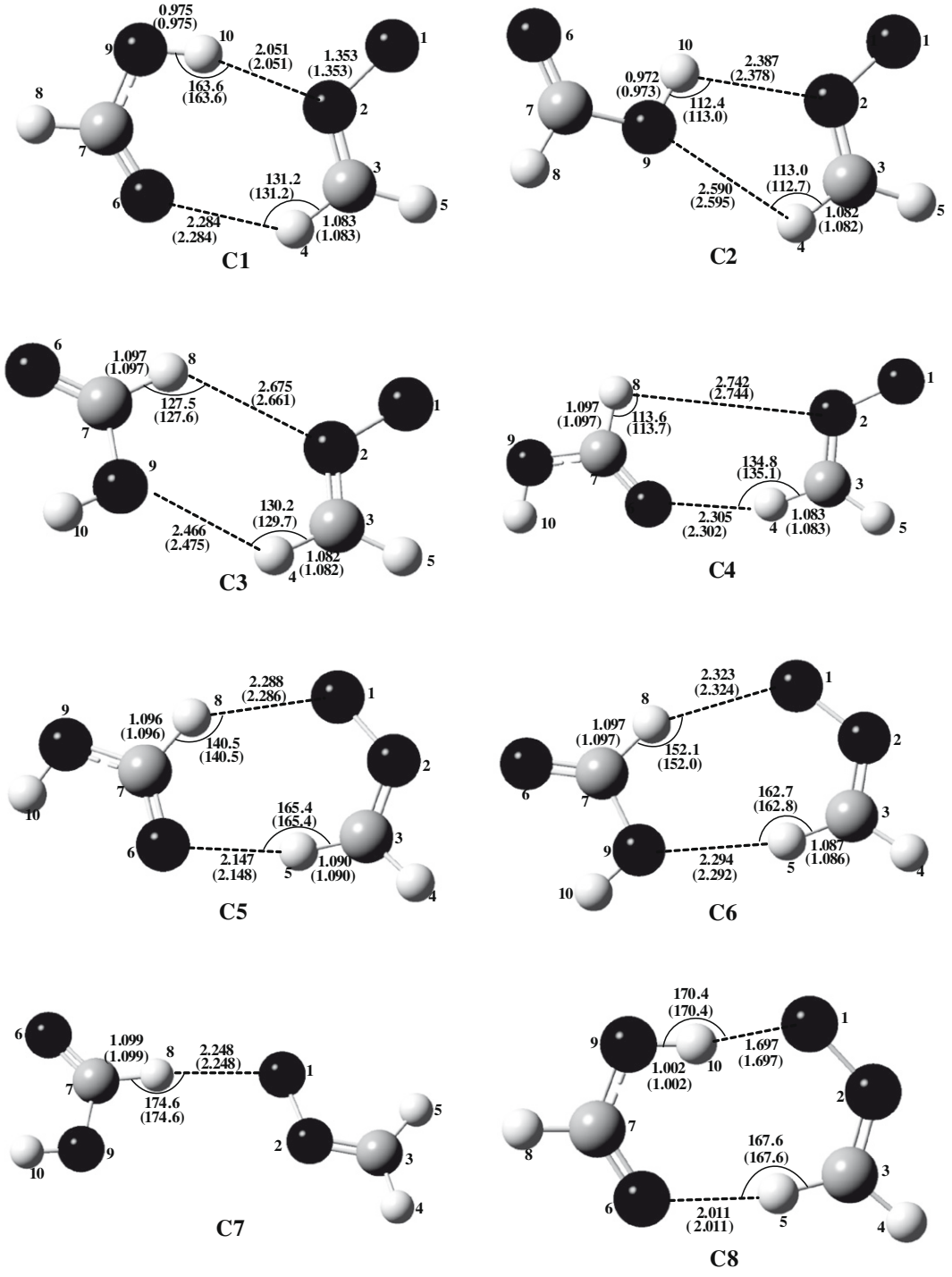

Fig. 1. The optimized geometries for the complexes formed between formic aid and carbonyl oxide at the B3LYP/6-311G(d,p), CBS-QB3 (in brackets) levels of theory (bond distances in angstroms and angles in degrees).

Table 1
The geometrical parameters for the complexes formed between HCOOH and H_2COO at the B3LYP/6-311G(d,p) level of theory (bond lengths in angstroms and angles in degrees).

Bond/angle	C1	C2	C3	C4	C5	C6	C7	C8	HCOOH	H2COO
O1O2	1.353	1.346	1.347	1.349	1.355	1.350	1.350	1.364		1.343
O2C3	1.261	1.261	1.260	1.260	1.258	1.259	1.257	1.255		1.260
C3H4	1.083	1.082	1.082	1.083	1.084	1.083	1.082	1.085		1.082
C3H5	1.085	1.085	1.085	1.085	1.090	1.087	1.085	1.093		1.085
O1O2C3	120.8	120.2	120.1	120.1	120.0	120.1	119.1	120.6		119.6
O2C3H4	114.3	114.9	114.7	114.5	114.1	114.5	115.3	113.6		115.4
O6C7	1.205	1.196	1.195	1.203	1.207	1.197	1.20	1.213	1.197	
C7H8	1.098	1.099	1.097	1.097	1.096	1.097	1.099	1.099	1.099	
C7O9	1.333	1.349	1.356	1.339	1.339	1.361	1.353	1.317	1.346	
O9H1O	0.975	0.972	0.971	0.971	120.2	0.970	0.970	1.002	0.970	
O6C7H8	124.1	125.6	118.7	125.2	124.3	127.5	126.5	122.6	125.6	
O6C7O9	126.0	125.2	124.2	124.6	123.9	123.5	123.8	126.5	125.2	
C7O9H1O	108.9	108.4	106.9	107.5	107.4	107.0	106.5	110.9	107.1	

of optimized geometries were computed at the same level to prove the characters of the transition states and the stationary points. In order to obtain the reliable relative energies, single-point energies were performed using the CCSD(T)/6-311++G(d,p) method at the B3LYP-optimized geometries. In these computations, the value of T1 diagnostic [26] in the CCSD wave function was considered to evaluate the reliability of these computations with respect to a possible multireference feature of the wave function at the stationary points. If the value of T1 diagnostic in the CCSD wave functions is larger than 0.44, the CCSD wave functions are thought not to be reliable according to Rienstra-Kiracofe et al. [27]. Moreover, as for the complexes founded in this study, the basis set superposition error (BSSE) was calculated using the counterpoise method by Boys and Bernardi [28] at the B3LYP/6-311G(d,p) level of theory to assess the energetic stability of the complexes better. In addition, the H-bond natures in this investigation were analyzed in terms of the atoms-in-molecules (AIM) theory by Bader [29]. If necessary, the intrinsic reaction coordinate (IRC) [30,31] was employed at the B3LYP/6-311G(d,p) level of theory to verify the connectivity between the transition states with the corresponding reactants and products.

Recent studies have indicated that the counterpoise (cp) method overestimates the BBSE [32–40]. However, the CBS-QB3 method is free of BSSE and computationally feasible for the complexes studied here. Moreover, there are some of authors who have reported [41–44,19] that reaction energies and barriers of the CBS-QB3 calculations are in well agreement with those of experimental results and greater accuracy than those of single-point CCSD(T) calculations with polarized triple-ζ basis sets. Thus, the CBS-QB3 method was applied to optimize all the stationary points as minima or saddle point and to calculate the frequencies of the corresponding stationary points for the reaction HCOOH and CH_2OO radical.

3. Results and discussions

3.1. The complexes formed between formic acid and carbonyl oxide

The purpose to search for the pre-complexes here is to assist to elucidate the reaction mechanisms. Thus, when the complexes are analyzed, we only take into account the factors relative to the binding energies. Due to the presence of both two hydrogen donors and two hydrogen acceptors in formic acid and carbonyl oxide, respectively, there are several complexes for them. As a result, eight complexes found in this study were displayed in Fig. 1. The optimized geometrical parameters for complexes and reactants are represented in Table 1 at the B3LYP/6-311G(d,p) level and are in agreement with the theoretical results [45–50] reported in the literature and experimental values [51]. Table 1 shows that the changes of the geometrical parameters of the complexes C8 are more obvious than those of corresponding reactants. Some of geometrical parameters of interest that characterize the H-bonds are provided in Fig. 1. It is worth nothing the geometrical parameters computed at the B3LYP/6-311G(d,p) level are exactly reproduced by employing the CBS-QB3 method. The T1 diagnostic is provided in Table 1 of supporting information, which the CCSD wave function was reliable in these computations. The relative energetic values of these complexes are listed in Table 2, which indicates that the binary complex C8 is lower in energy than others. Additionally, from Table 1, it is found that the CP method correction is not adequate for complexes C1, C5, C6 and C8, comparing the calculated results by CBS-QB3 method.

From the geometrical point of view, the strength of the H-bond between a proton donor X···H and a proton acceptor Y is determined by its length, the bond length of the H—Y, the lengthening of X—H, the bond length X—H vs H—Y and its angles, which is reported by Steiner [52]. The expectation is confirmed by that the intermolecular R(O—H) distance listed in part C8 of Fig. 1 is in accordance with the notion that the OH—O hydrogen bond and CH—O hydrogen bond are stronger and shorter than their OH—O and CH—O counterparts. Additionally, the O9H10 bond to stretch in complexes C8 is the largest than those of other complexes, which is again reflected the H-bond strength. It is also evident that the OH—O bond distances in complexes C1, C2, C8 are shorter than their corresponding CH—O distances. In addition, one can observe the tendency that the oxygen atom without lone pain electron as a proton acceptor leads to the weak hydrogen bond, especially in complexes C2, C3. The bond angles of the O9H10O2, O9H4C3 in complex C2 and the C7H8O2 in complex C4 are smaller than those of other hydrogen bonds, which reflects that the bonds are weaker.

The quantum theory of atoms-in-molecules is powerful tool to analyze the bonding nature, as proposed by Bader [29]. Moreover,

Table 2
The relative enthalpies the binding energies of the complexes formed between H_2COO and HCOOH with zero-point correction included (kcal/mol) at 298.15 K.*

Complexes	B3LYP				CBS-QB3	
	ΔH^a	ΔE^a	ΔE^b	Δe^c	ΔH^d	ΔE^d
C1	−5.7	−6.0	−5.6	−3.5	−5.7	−5.1
C2	−1.7	−2.3	−2.8	−1.7	−2.1	−1.5
C3	−1.5	−2.1	−2.7	−1.6	−1.9	−1.3
C4	−3.4	−4.0	−4.1	−2.5	−3.7	−3.1
C5	−6.1	−6.4	−5.2	−2.9	−5.5	−4.9
C6	−3.7	−4.2	−3.6	−1.7	−3.3	−2.7
C7	−2.7	−3.4	−3.0	−1.6	−2.4	−1.8
C8	−13.7	−13.7	−10.6	−7.5	−11.6	−11

* The relative enthalpies and the binding energies are computed at the a, B3LYP/6-311G(d,p); b, CCSD(T)/6-311++G(d,p)//B3LYP/6-311G(d,p) levels; c, the values with BSSE were calculated at the CCSD(T)/6-311++G(d,p)//B3LYP/6-311G(d,p); d, the values are obtained at the CBS-QB3 level of theory.

Table 3
Topological properties of the bond critical points for the complex formed between HCOOH and H2COO radical at the B3LYP/6-311G(d,p) level of theory.*

Complexes	Bond	Δr (Å)[a]	Bond	ρ (au)[b]	$\Delta^2\rho$(au)[c]	(ε)[d]
C1	O9H10	0.005	H10O2	0.0183	0.0687	0.0411
	C3H4	0.001	O6H4	0.0136	0.0479	0.0563
C2	O9H10	0.002	H10O2	0.0104	0.0403	0.2032
	C3H4	0.000	O9H4	0.0073	0.0279	0.2463
C3	C7H8	−0.002	H8O2	0.0061	0.0205	0.0276
	C3H4	0.000	O9H4	0.0092	0.0315	0.0409
C4	C7H8	−0.002	H8O2	0.0055	0.0204	0.1812
	C3H4	0.001	O6H4	0.0131	0.0441	0.0125
C5	C7H8	−0.003	H8O1	0.0175	0.0576	0.0274
	C3H5	0.005	O6H5	0.0144	0.0442	0.0394
C6	C7H8	−0.002	H8O1	0.0131	0.0389	0.0562
	C3H5	0.002	O9H5	0.0120	0.0407	0.0824
C7	C7H8	0.000	H8O1	0.0152	0.0458	0.0908
C8	O9H10	0.032	H10O1	0.0456	0.1266	0.0735
	C3H5	0.008	O6H5	0.0232	0.0801	0.0106

* a, The bond length differences between the complexes and the corresponding reactants; b, electron charge density at the bond critical points; c, Laplacian of the electron density at the bond critical points; d, the ellipticity at bond critical point.

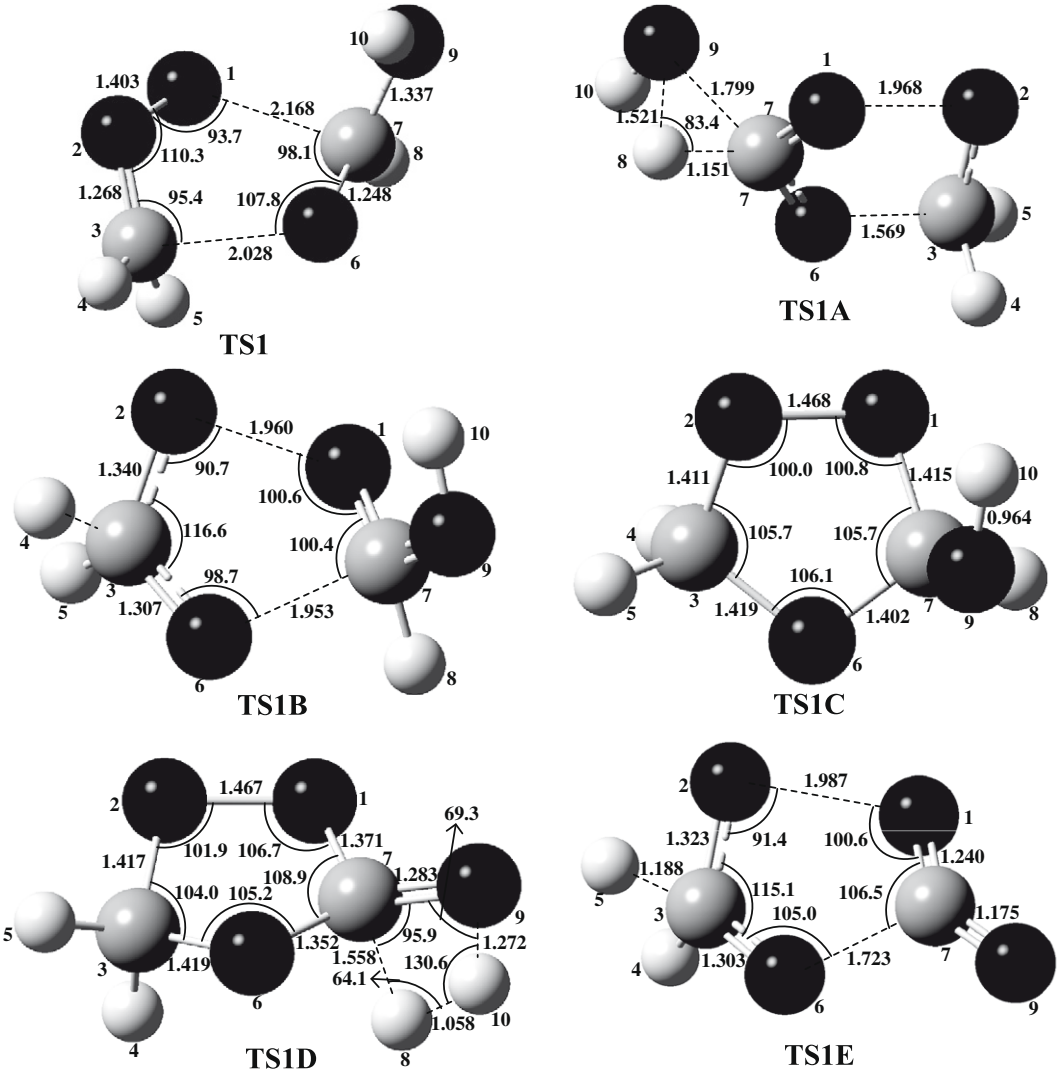

Fig. 2. The optimized geometries of transition states at the B3LYP/6-311G(d,p) level of theory.

in terms of the AIM theory, Koch and Popelier [53] provided a set of criteria to full describe the hydrogen bond interactions. The electron density and the Laplacian of the electron density at the bond critical points correlate the H-bond strength, which is focused here to clarify the binding energies and thus further help elucidate the reaction mechanism. The electron density at the bcp's reported in the next five column in Table 3 clearly reveals the notion that the electron density can reflect the H-bond strength. The electron density ($\rho_{H10O1} = 0.0456$ and $\rho_{H5C3} = 0.0232$) at the H10O1's and the H5C3's in C8 are larger in magnitude than those of corresponding bond critical points, which is relative to the strongest binding energy. Once again, the OH—O hydrogen bonds in complexes C1, C2, C8 are stronger than the CH—O hydrogen bond, which is confirm by the electron density provided in Table 3. Additionally, the electron densities ($\rho_{H8O2} < \rho_{O6H4}$ in C4 and $\rho_{H8O1} > \rho_{O9H5}$ in C6) again verify the tendency that oxygen atom with lone pain electrons cause the weak hydrogen bond, which is mentioned above, whereas the situation ($\rho_{H10O2} > \rho_{O6H2}$) in complex C1 is different which shows that OH—O bond is stronger. The ellipticity, ε, measures not only the π character of a bond but also the bond strength. The value is large, which represents the weak bond. In Table 3, the values of the H10O2, H4C3 in complex C2 and H8O2 in complex C4 are larger than those of other hydrogen bonds, which the hydrogen bonds are weaker.

3.2. The concerted reactions between formic acid and carbonyl oxide

The initial reactions formic acid with carbonyl oxide are displayed in Eqs. (1) and (4), which is proposed by Neeb et al. [11] and Aplincourt and Ruiz-lopez [24]. There are two reaction channels leading to the formation of the transitory products, hydroxylated ozonide and hydroperoxymethyl formate, which are taken into account in this study.

The first elementary reaction through TS1 depicted in part TS1 of Fig. 2 is that the terminal oxygen atom and the carbon oxygen in CH_2OO simultaneously attack the C=O bond of the formic acid to form the hydroxylated ozonide (P1) provided in Fig. 4. The reaction mechanism is similar to the reaction formaldehyde with carbonyl oxide reported in the literatures [24,50]. The changes that O1O2, O2C3, O6C7 bond distances in TS1 are lengthened are 0.060 Å, 0.008 Å, 0.051 Å, respectively, whereas the changes of the C7O9 and C7H8 bond distances contracted are 0.009 Å and 0.011 Å, respectively. As formic acid and carbonyl oxide further approach, the bond lengths of the O1C7 and C3O6 are shortened and the bond distances of O1O2, O2C3 and O6C7 are lengthened. The calculated potential energy profile is given in Fig. 5 at the CBS-QB3 level of theory. The barrier height through TS1 presented in Table 4 is 2.8 kcal/mol, −0.5 kcal/mol at the CCSD(T)/6-311++G(d,p)//B3LYP/6-311G(d,p), CBS-QB3 levels, which indicates

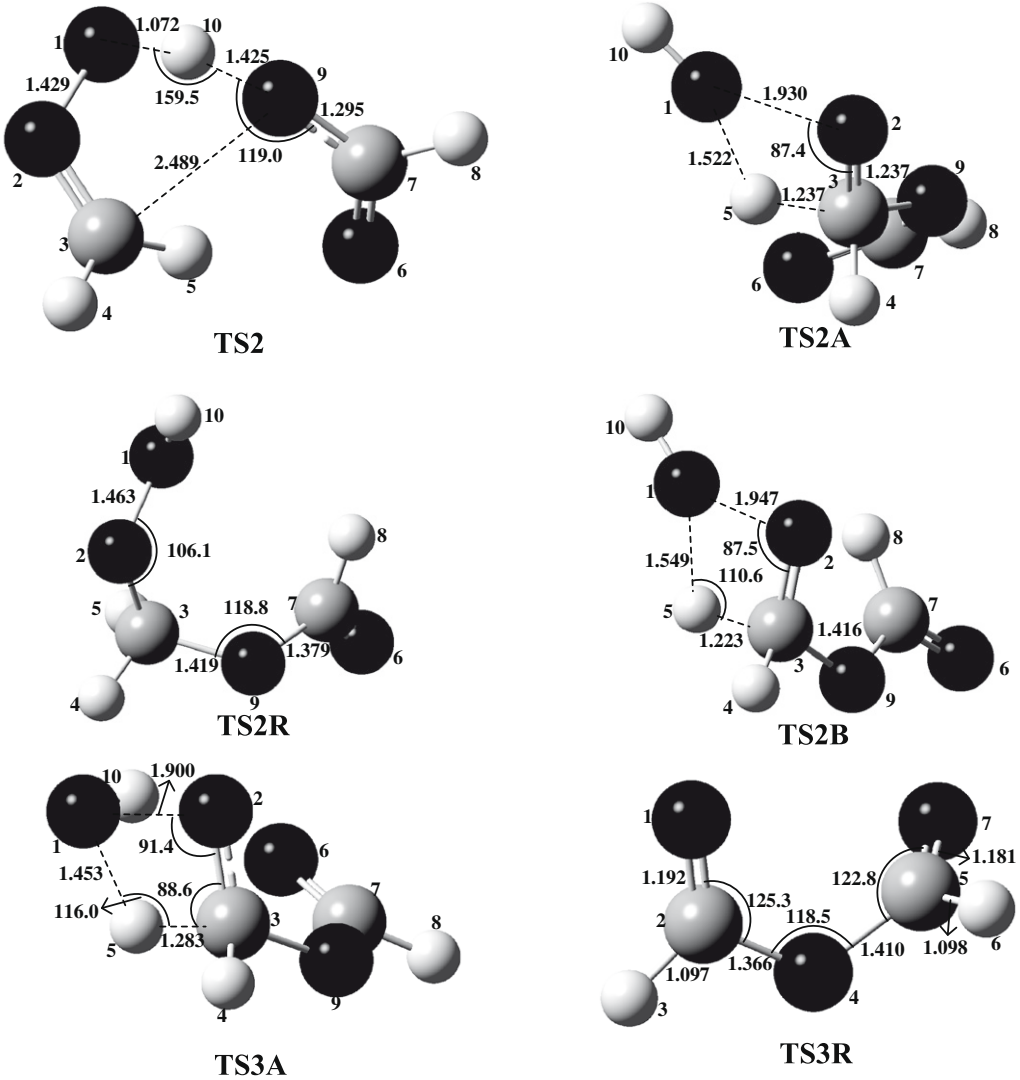

Fig. 3. The optimized geometries of transition states at the B3LYP/6-311G(d,p) level of theory.

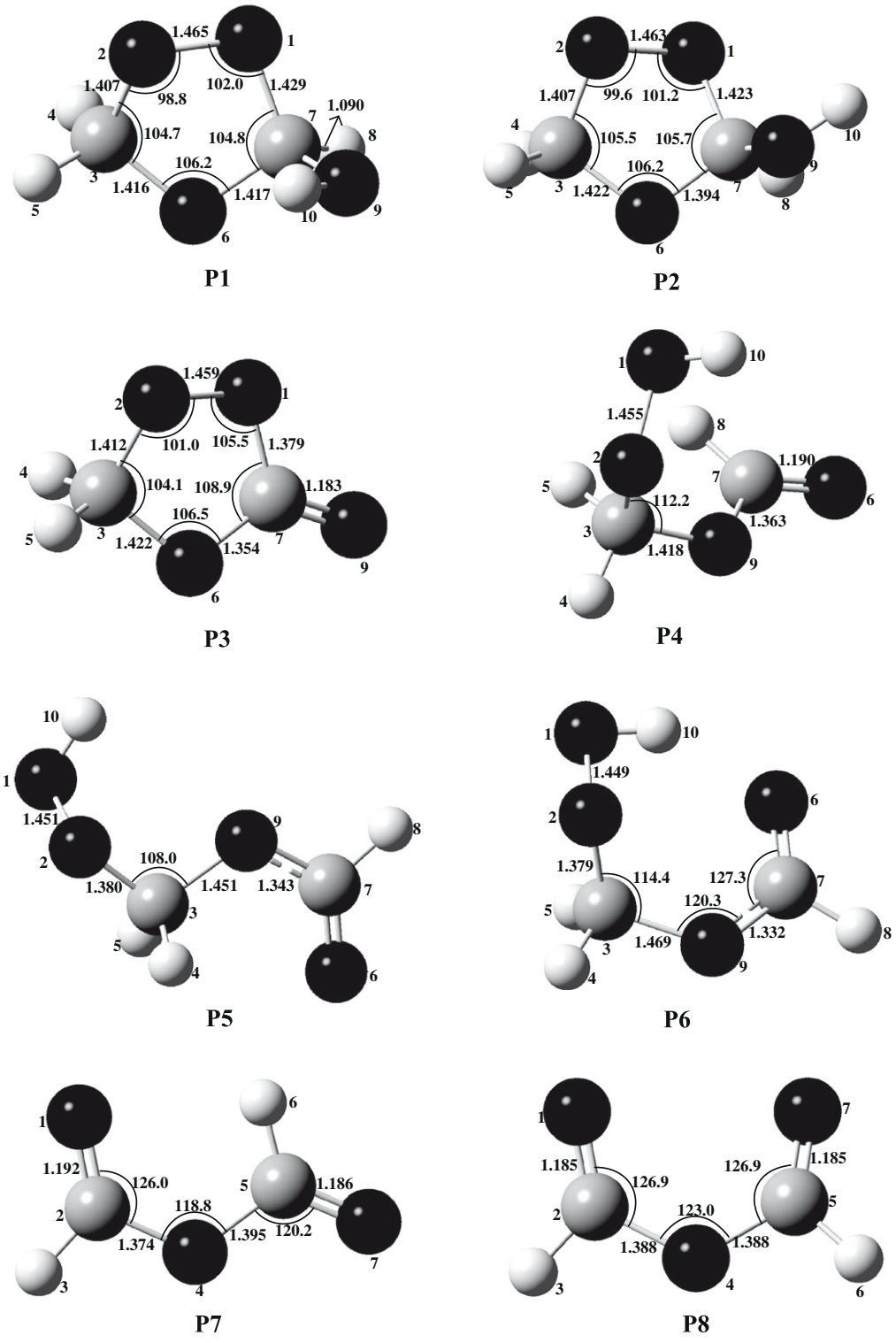

Fig. 4. The optimized geometries of transition states at the B3LYP/6-311(d,p) level of theory.

that the reaction by TS1 is quite feasible, as compared with the energy barrier 2.3 kcal/mol of the reaction carbonyl oxide with water [50]. The change of the reaction enthalpy for TS1 is −41.3 kcal/mol as given in Table 4 at the CBS-QB3 level of theory, implying that the reaction is an exoergic reaction.

The other reaction pathway (TS2) displayed in part TS2 of Fig. 3 is that the hydrogen atom in OH of the formic acid is transferred to the terminal oxygen atom of the carbonyl oxide and simultaneously the oxygen atom of the OH is added to the carbon atom of the carbonyl oxide responsible for the formation of the hydroperoxymethyl formate. As for the hydroperoxymethyl formate, three distinct conformers exist as provided in part P4, P5 and P6 of Fig. 4. Because of the presence of the intramolecule hydrogen bond, the P6 conformer is the most stable, which is verified by experimental

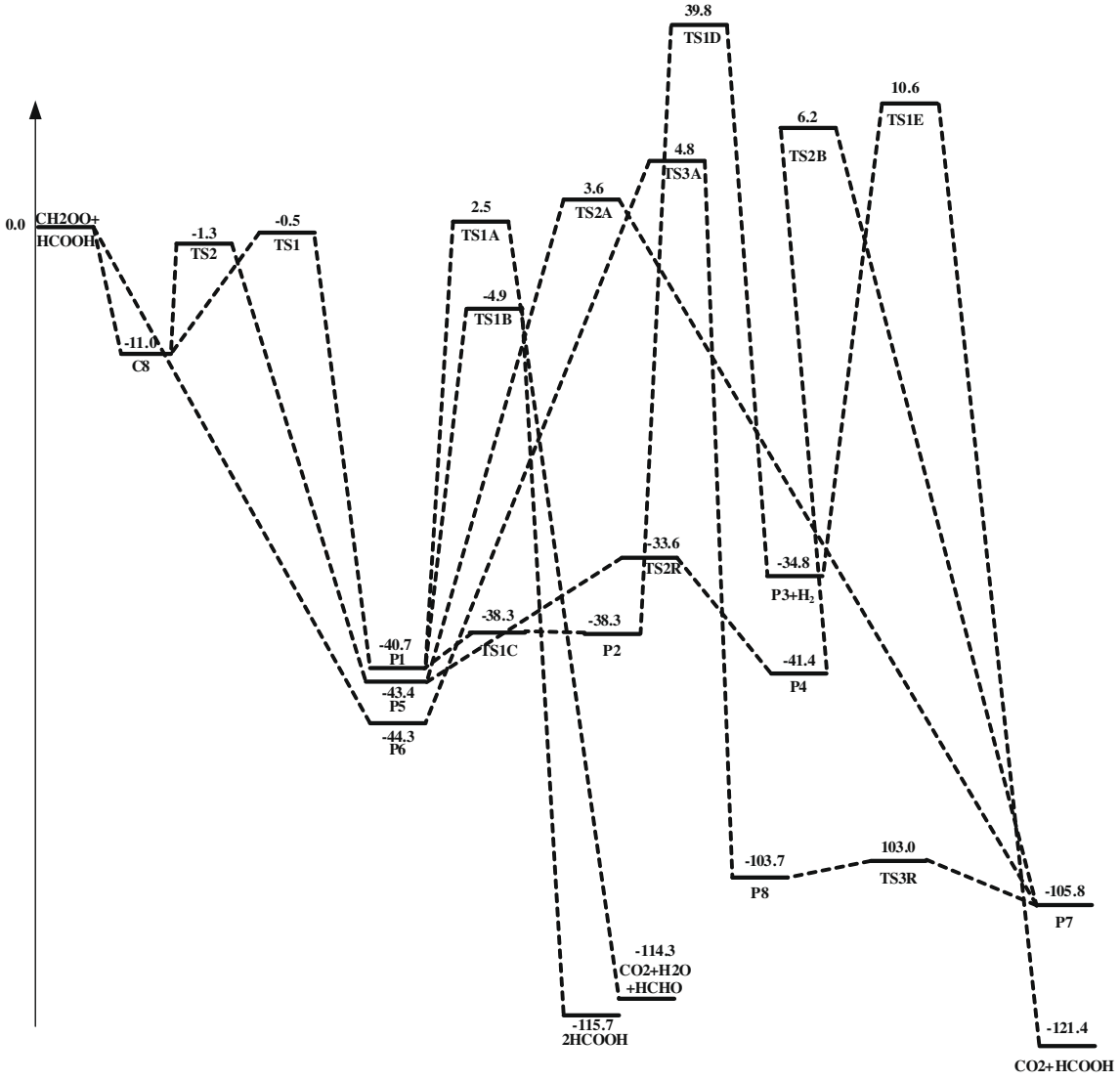

Fig. 5. The calculated potential energy profile at the CBS-QB3 level of theory.

results [23]. However, the theoretical prediction shows that the reaction energy for P6 minus P5 is 0.1 kcal/mol, −0.9 kcal/mol at the CCSD(T/6-311++G(d,)p)//B3LYP/6-311G(d,p), CBS-QB3 levels, which proves that the CBS-QB3 theoretical method can better char-

Table 4
The calculated activated energies, enthalpies and reaction energies for the reaction between H_2COO and HCOOH.*

	Energy reference	Activated energies				Reaction energies			
		B3LYP		CBS-QB3		B3LYP		CBS-QB3	
		ΔH^a	ΔE^a	ΔH^b	ΔE^b	ΔH^a	ΔE^a	ΔH^b	ΔE^b
TS1	R[c]	−0.3	2.8	−1.1	−0.5	32.9	−36.0	−41.3	−40.7
TS2	R[c]	−4.0	1.1	−1.8	−1.3	−40.6	−42.0	−44.0	−43.4
TS1A	P1	54.9	58.0	43.2	43.2	−77.3	−84.1	−71.9	−73.6
TS1B	P1	30.6	33.5	35.8	35.8	−82.1	−81.0	−74.4	−75.0
TS1C	P1	2.7	2.8	2.4	2.4	2.7	2.4	2.4	2.4
TS1D	P2	73.5	79.0	78.1	78.1	2.6	2.5	4.1	3.5
TS1E	P3	37.4	41.4	45.4	45.4	−92.2	−94.5	−85.9	−86.5
TS2A	P5	46.7	44.8	47	47	−60.3	−66.2	−62.6	−63.1
TS2R	P5	9.6	9.6	9.8	9.8	2.1	2.1	2.0	2.0
TS2B	P4	47.2	45.4	47.6	47.6	−62.4	−68.3	−64.5	−65.1
TS3	R	–	–	–	–	−42.7	−41.9	−44.8	−44.3
TS3A	P6	48.5	46.8	49.1	49.1	−55.7	−64.0	−58.8	−59.4
TS3R	P8	1.7	1.3	0.7	0.7	−2.5	−2.2	−2.9	−2.9

* a, The AH is computed at the B3LYP/6-311G(d,p) level of theory; the AE is calculated at the CCSD(T)/6-311++G(d,p)//B3LYP/6-311G(d,p) computational level; b, AH and AE are obtained at the CBS-QB3 level of theory; c, R represents the reactants, including the HCOOH and H_2COO.

acterize the products in terms of experimental values [23] that the P6 product is lower 1–2 kcal/mol in energy than those of P4 and P5. The expectation is confirmed by the energetic difference between P4 and P5 as listed in the next ten row of Table 4.

The only one transition state in this study was found to lead to the formation of the product (P5). The intrinsic reaction coordinate (IRC) is applied here to confirm the product (P5) corresponding the transition state (TS2). The O9H10 bond length in TS2 is longer by 0.455 Å in the formic acid' counterpart, whereas the change of the O9C7 bond distance shortened in TS2 is 0.059 Å. Although the calculated results demonstrate that the reaction by the transition state (TS2) is more reactive than one of TS1, which is confirmed by the change of the reaction enthalpy and the barrier height for TS2 that are lower 3.7 kcal/mol and 0.8 kcal/mol than those of the TS1 at the CBS-QB3 level of theory, the energy barriers of the two pathways using the two different methods are less than 3 kcal/mol, which contributes to the initial reaction. In addition, we assume that the product (P4) is produced through the internal rotation around the C3O9 bond of P5. The corresponding transition state (TS2R) is also located as displayed in Fig. 3. The reaction energy is 2.0 kcal/mol, which agrees with the theoretical prediction [24]. The energy barrier for TS2R is 9.6 kcal/mol, 9.8 kcal/mol at the different levels, which the two methods are in good agreements. The high barrier of the internal rotation is caused by the repulsive force between H8 and H10. However, as for the product (P6), we presume that the reaction is likely to be barrierless.

3.3. The splits of the hydroxylated ozonide and hydroperoxymethyl formate

The dissociation reactions for the transitory products are quite complex. Thus, as for hydroxylated ozonide, there are three reaction pathways considered that are result in the formation of the fragments. The one reaction channel (TS1A) simultaneously undergoes the splits of O1O2 bond and C3O6 bond and C7H8 bond and C7O9 to result in the formation water, CO_2 and HCOH as shown in Fig. 2. The other reaction pathway (TS1B) is responsible for the formation of the formic acid by the way of the simultaneous cleavages of O1O2 bond, C1O6 bond and C3H4 bond as presented in part TS1B of Fig. 2. Since the reactants contain the formic acid and the unimolecular reaction of the excited carbonyl oxide can produce the water, CO_2 and HCHO and so on, there is difficulty in detecting the reaction system. Thus, the theoretical computation is preferable to clarify the reaction mechanisms of transitory product (hydroxylated ozonide). The computational studies indicate that the unimolecular decomposition reaction is more feasible through TS1B than that of TS1A, for the energy barrier by TS1A is higher 8.4 kcal/mol than the corresponding TS1B. The third reaction pathway via the transition state TS1C is that the hydrogen atom (H10) undergoes the internal rotation around the C7O9 single bond responsible for the formation of P2, which subsequently decomposes into H_2 and P3 through the transition TS1D. Finally, the cyclic product P3 by the TS1E undergoes unimolecular decomposition to yield the formation of CO_2 and HCOOH, which has been investigated by Aplincourt [50]. In Table 4, the activated barrier via TS1C is 2.4–2.7 kcal/mol, showing that internal rotation reaction is preferable. However, the energy barrier for TS1D is so high that it is difficult to occur in the atmospheric condition.

The decompositions of the hydroperoxymethyl formate including the transitory products (P4, P5 and P6) occur via the scissions of the C3H5 bond and O1O2 bond responsible for the formation of water and anti-formic acid anhydride or syn-formic acid anhydride. The transitory products of P5, P6 undergo the unimolecular reactions to form the syn-formic acid anhydride and water through TS2A and TS3A in Fig. 3, respectively, while the P4 via TS2B is responsible for the formation of anti-formic acid anhydride and water. The theoretical calculations show that although the barriers of the three reaction pathways responsible for the splits of the hydroperoxymethyl formate are different at the different methods, the barriers are approximately equal for the three pathways at the same theoretical method. The computational results show that the barrier of the unimolecular decomposition through TS1B is lower 6.4–13.3 kcal/mol than the rest of the split of the hydroxylated ozonide and hydroperoxymethyl formate.

There are two different conformers for formic acid anhydride. The experimental investigation [23] has led to the conclusion that the syn-formic acid anhydride (P7) is more stationary than anti-formic acid anhydride (P8). To elucidate the reaction mechanisms, the transformation the anti-formic acid anhydride to syn-formic acid anhydride is considered and the corresponding transition state by TS3R is found as depicted in Fig. 3. The theoretical studies imply that the interconversion between the distinct conformers is quite feasible, for the barrier height is 0.7 kcal/mol at the CBS-QB3 level of theory. Thus, the mainly final product of the reaction carbonyl oxide with formic acid is anti-formic acid anhydride, which is confirmed by experimental results [23].

4. Conclusions

The quantum chemical methods are employed to investigate the reactions carbonyl oxide with formic oxide. The calculated results indicate that the first step is that the H-bond complexes are formed between H2COO and HCOOH. The binding energy of the most stationary complex is 11.0 kcal/mol at the CBS-QB3 level of theory, which plays an important role in the reaction carbonyl oxide with formic acid. In addition, the two transition states for the initial reactions CH_2OO with HCOOH also located, whose activated energies are −0.5 kcal/mol and −1.3 kcal/mol, respectively, which shows that the two reaction channels are significant for the starting reaction carbonyl oxide with formic acid. Finally, the splits of hydroxylated ozonide and hydroperoxymethyl formate are quite difficult due to the barriers by 35.8–49.1 kcal/mol at the CBS-QB3 level of theory under the atmospheric conditions. However, if under some conditions the splits of hydroxylated ozonide and hydroperoxymethyl formate can occur, the mainly final products are anti-formic acid anhydride and formic acid. It is worth to note that formic acid is produced in the reaction carbonyl oxide with formic acid under some conditions.

References

[1] R.P. Wayne, Chemistry of Atmospheres, third ed., Oxford University Press, Oxford, 2000.
[2] R. Gutbrod, E. Kraka, R.N. Schindler, D. Cremer, J. Am. Chem. Soc. 119 (1997) 732.
[3] M. Olzmann, E. Kraka, D. Cremer, R. Gutbrod, S. Andersson, J. Phys. Chem. A 101 (1997) 9421.
[4] D. Cremer, J. Gauss, E. Kraka, J.F. Stanton, R.J. Bartlett, Chem. Phys. Lett. 209 (1993) 547.
[5] R. Atkinson, S.M. Aschmann, Environ. Sci. Technol. 27 (1993) 1357.
[6] O. Horie, G.K. Moortgat, Atmos. Environ. A 25 (1991) 1881.
[7] F. Su, J.G. Calvert, J.H. Shaw, J. Phys. Chem. 84 (1980) 239.
[8] H. Niki, P.D. Maker, C.M. Savage, P.L. Breitenbach, J. Phys. Chem. 85 (1981) 1024.
[9] S. Hatakeyama, H. Kobayashi, H. Akimoto, J. Phys. Chem. 88 (1984) 4736.
[10] P. Neeb, O. Horie, G.K. Moortgat, J. Phys. Chem. A 102 (1998) 6778.
[11] P. Neeb, O. Horie, G.K. Moortgat, Atmos. Environ. 31 (1997) 1417.
[12] H.J. Tobias, P.J. Ziemann, J. Phys. Chem. A 105 (2001) 6129.
[13] B. Bonn, G. Schuster, G.K. Moortgat, J. Phys. Chem. A 106 (2002) 2869.
[14] S. Hatakeyama, H. Akimoto, Res. Chem. Intermed. 20 (1994) 503.
[15] O. Horie, P. Neeb, G.K. Moortgat, Int. J. Chem. Kinet. 29 (1997) 461.
[16] J.D. Fenske, A.L. Hasson, A.W. Ho, S.E. Paulson, J. Phys. Chem. A 104 (2000) 9921.
[17] R. Crehuet, J.M. Anglada, J.M. Bofill, Chem. Eur. J. 7 (10) (2001) 2227.
[18] J.M. Anglada, P. Aplincourt, J.M. Bofill, D. Cremer, Chem. Phys. Chem. 2 (2002) 215.

[19] A.S. Hasson, M.Y. Chung, K.T. Kuwata, A.D. Converse, D. Krohn, S.E. Paulson, J. Phys. Chem. A 107 (2003) 6176.
[20] P. Aplincourt, J.M. Anglada, J. Phys. Chem. A 107 (2003) 5798.
[21] G. Orzechowska, S.E. Paulson, J. Phys. Chem. A 109 (2005) 5358.
[22] R. Criegee, Angew. Chem. Int. Ed. 14 (11) (1975) 745.
[23] P. Neeb, O. Horie, G.K. Moortgat, Chem. Phys. Lett. 246 (1995) 150.
[24] P. Aplincourt, M.F. Ruiz-lopez, J. Phys. Chem. A 104 (2000) 380.
[25] M.J. Frisch, G.W. Trucks, H.B. Schlegel, G.E. Scuseria, M.A. Robb, J.R. Cheeseman, Gaussian 03, Revision A01, Gaussian Inc., Wallingford, CT, 2003.
[26] T.J. Lee, P.R. Taylor, Int. J. Quant. Chem. Symp. 23 (1989) 199.
[27] J.C. Rienstra-Kiracofe, W.D. Allen, H.F. Schaefer, J. Phys. Chem. A. 104 (2000) 9823.
[28] S.F. Boys, F. Bernardi, Mol. Phys. 19 (1970) 553.
[29] R.F.W. Bader, Chem. Rev. 91 (1991) 893.
[30] C. Gonzalez, H.B. Schlegel, J. Phys. Chem. 94 (1990) 5523.
[31] C. Gonzalez, H.B. Schlegel, J. Phys. Chem. 90 (1989) 2154.
[32] A. Johansson, P. Kollman, S. Rothenberg, Theor. Chim. Acta 29 (1973) 167.
[33] J.P. Daudey, P. Claveriand, J.P. Malrieu, Int. J. Quant. Chem. 8 (1974) 1.
[34] M.J. Frisch, J.E. Del Bene, J.S. Binkley, H.F. Schaefer, J. Chem. Phys. 84 (1986) 2279.
[35] D.W. Schwenke, D.G. Truhlar, J. Chem. Phys. 82 (1985) 2418.
[36] K. Morokuma, K. Kitaura, in: P. Politzer (Ed.), Chemical Application of Atomic and Molecular Electronic Potentials, Plenum, New York, 1981.
[37] J.C. Lupez, J.L. Alonso, F.J. Lorenzo, V.M. Rayon, J.A. Sordo, J. Chem. Phys. 111 (1999) 6363.
[38] S.W. Hunt, K.R. Leopold, J. Phys. Chem. A 105 (2001) 5498.
[39] H. Valdvs, J.A. Sordo, J. Comput. Chem. 23 (2002) 444.
[40] H. Valdvs, J.A. Sordo, J. Phys. Chem. A 106 (2002) 3690.
[41] R. Gomez-Balderas, M.L. Coote, D.J. Henry, L. Radom, J. Phys. Chem. A 108 (2004) 2874.
[42] D.J. Henry, C.J. Parkinson, L. Radom, J. Phys. Chem. A 106 (2002) 7927.
[43] V. Guner, K.S. Khuong, A.G. Leach, P.S. Lee, M.D. Bartberger, K.N. Houk, J. Phys. Chem. A 107 (2003) 11445.
[44] K.T. Kuwata, A.S. Hasson, R.V. Dickinson, E.B. Petersen, L.C. Valin, J. Phys. Chem. A 109 (2005) 2514.
[45] A. Andersen, E.A. Carter, J. Phys. Chem. A 107 (2003) 9463.
[46] A. Alparone, A. Millefiori, S. Millefiori, Chem. Phys. Lett. 409 (2005) 288.
[47] R.W. Gora, S.J. Grabowski, J. Leszczynski, J. Phys. Chem. A 109 (2005) 6397.
[48] M.T. Sucarrat, J.M. Anglada, J. Phys. Chem. A 110 (2006) 9718.
[49] A. Mansergas, J.M. Anglada, J. Phys. Chem. A 110 (2006) 4001.
[50] P. Aplincourt, M.F. Ruiz-Lopez, J. Am. Chem. Soc. 122 (2000) 8990.
[51] E. Bjarnow, W.M. Hocking, Z. Naturforsch. 33A (1978) 610.
[52] T. Steiner, Angew. Chem. Int. Ed. 41 (2002) 48.
[53] U. Koch, P.L.A. Popelier, J. Phys. Chem. 99 (1995) 9747.